

Modulated Contrast and Associated Diffracted Intensity of GaP_ySb_{1-y} Layers Grown Using Organometallic Vapor Phase Epitaxy

Tae-Yeon SEONG*

Department of Materials Science and Engineering, Korea University, Seoul 136-713

G. R. BOOKER

Department of Materials, University of Oxford, Parks Road, Oxford OX1 3PH, U.K.

A. G. NORMAN

National Renewable Energy Laboratory, 1617 Cole Boulevard, Golden, Colorado 80401-3393, U.S.A.

F. GLAS

*France Telecom, Centre National d'Etudes des Telecommunications, Paris, B,
Lab de Bagneux, 196 Ave Henri Ravera, BP 107, 92225 Bagneux, France*

G. B. STRINGFELLOW

*Department of Materials Science and Engineering,
University of Utah, Salt Lake City, Utah 84112, U.S.A.*

(Received 20 November 2007)

We have investigated the modulated structures and its associated diffracted diffuse intensity, of organometallic vapor phase epitaxially grown GaPSb (001) layers by using transmission electron microscopy (TEM) and transmission electron diffraction (TED). The TEM results reveal the co-existence of a fine-scale modulated contrast and a fine-scale speckled contrast. In addition, a fine needle-like contrast is observed. The [001] TED results show lines of [110]-oriented diffuse intensity diffuse streaks passing through the fundamental reflections, satellite spots at $1/4g[220]$ positions, and a [010]-oriented diffuse intensity with spacing of $1/6g[040]$. Simulations using the Valence Force Field model were performed to understand the origin of the diffracted features. The observed distributions of diffuse intensity are shown to be partially consistent with random disorder. Furthermore, the [110]-oriented diffuse lines are attributed to a static displacement of the sites of the mixed sublattices.

PACS numbers: 81.05.Ea

Keywords: Modulated structures, Diffracted intensity

I. INTRODUCTION

III-V compound semiconductor epitaxial layers are of importance for various applications in optoelectronic devices, such as laser diodes and photo-detectors [1, 2]. Growth of uniform epitaxial layers of ternary and quaternary III-V semiconductors is sometimes difficult for certain alloy composition and temperatures due to the presence of miscibility gaps [3–6]. However, non-equilibrium growth techniques, such as organometallic vapor phase epitaxy (OMVPE) and molecular beam epitaxy (MBE), have been used to grow good quality epitaxial layers of such semiconductors.

Electron microscopy results showed the presence of a fine modulated contrast attributed to alloy clustering possibly occurring as a result of spinodal decomposition in epitaxial III-V compound semiconductor layers [7–10, 12]. It was shown that there are two different kinds of modulated structures, one giving a coarse-scale tweed-like contrast with a periodicity of 100 – 200 nm, and the other a quasi-periodic fine-scale contrast with a periodicity of ~ 10 nm. For example, Blood and Grassie [13] reported calculations based on previously published structural data, showing that the conduction band in GaInAsP alloys had a spatial variation with an amplitude of ~ 0.08 eV and that such a variation could result from partial segregation into clusters. The effects of alloy clustering on the photoluminescence properties

*E-mail: tyseong@korea.ac.kr

Table 1. Growth conditions for epitaxial $\text{GaP}_y\text{Sb}_{1-y}$ OMVPE layers.

Sample No.	$\text{GaP}_y\text{Sb}_{1-y}$ (y)	Growth temp. ($^{\circ}\text{C}$)	Growth rate (nm/s)
3-38	0.58	500	0.24
3-37	0.59	530	0.76
3-23	0.51	560	0.28
3-24	0.75	560	0.56
3-44	0.77	600	1.46

of GaInP was also described, and it was argued that alloy clustering due to spinodal decomposition during the growth process might have an adverse effect on both the electrical and optical properties of the layers [13,14]. So far, detailed structural investigations have not been widely performed on GaPSb layers to date. In this work, we present transmission electron microscopy (TEM) and transmission electron diffraction (TED) examinations of the modulated structure and diffracted diffuse intensity of GaPSb layers grown by OMVPE.

II. EXPERIMENT

The OMVPE growth was carried out in an atmospheric-pressure, horizontal, infrared-heated reactor [15]. The reactants were trimethylgallium (TMGa) and trimethylantimony (TMSb) held in temperature controlled bubblers at -12 and 11 $^{\circ}\text{C}$, respectively, and phosphine consisting of a 10 % mixture in Pd-diffused H_2 . The molar flow rates were varied in the following ranges: $f_{\text{TMGa}} = 1.92 - 2.88 \times 10^{-5}$ mol/min, $f_{\text{TMSb}} = 3.37 - 7.02 \times 10^{-5}$ mol/min, and $f_{\text{PH}_3} = 0.83 - 4.16 \times 10^{-5}$ mol/min. The layer composition $\text{GaP}_y\text{Sb}_{1-y}$ was varied from $y = 0.51$ to 0.77 , the growth temperature between 500 and 600 $^{\circ}\text{C}$, and growth rate between 0.24 and 1.46 nm/s. The layers were grown on (001) GaAs substrates. The details of the layers examined are listed in Table 1.

(001) plan-view and $\{110\}$ cross-sectional TEM specimens were prepared using standard techniques and the thinned materials were examined using a JEOL 4000EX electron microscope operated at 400 kV. The convergent beam electron diffraction (CBED) technique [16] was used to determine the polarity between the $[110]$ and $[-110]$ directions. The polarity of the GaPSb layers was assumed to be the same as that of the underlying GaAs substrate.

III. RESULTS AND DISCUSSION

TEM dark-field (DF) investigations using $\mathbf{g}\langle 220 \rangle$ and $\mathbf{g}\langle 400 \rangle$ reflections were carried out on $[001]$ plan-view

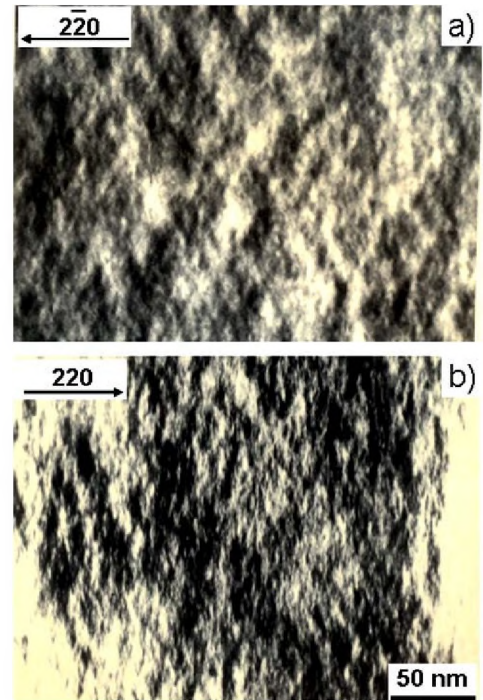


Fig. 1. (a) $[110]$ cross-sectional ($2\bar{2}0$) and (b) $[-110]$ cross-sectional (220) TEM DF images from an $\text{InP}_{0.59}\text{Sb}_{0.41}$ layer grown at 470 $^{\circ}\text{C}$ and 0.55 nm/s.

and $\langle 110 \rangle$ cross-sectional specimens to investigate the microstructure of the $\text{GaP}_y\text{Sb}_{1-y}$ layers. The examinations showed a quasi-periodic fine-scale modulated contrast similar to that previously observed in $\text{InP}_y\text{Sb}_{1-y}$ layer [17] and attributed to alloy clustering due to spinodal decomposition occurring at the growing surface during layer growth. A quasi-periodic fine needle-like contrast also occurred, which was also observed in the $\text{InP}_y\text{Sb}_{1-y}$ layers and was attributed to segregation of atoms associated with rows of missing dimmers present in the reconstructed surface during growth. For example, $\langle 220 \rangle$ cross-sectional DF images of an $\text{InP}_{0.59}\text{Sb}_{0.41}$ layer grown at 470 $^{\circ}\text{C}$ and 0.56 nm/s are shown in Figure 1 [17]. The DF images exhibit the co-existence of a fine-scale modulated contrast ($15 - 20$ nm) and a fine-scale speckled contrast (~ 5 nm) in both the $[110]$ and the $[-110]$ cross-sectional samples. For the $[-110]$ cross-sectional sample, however, the DF image taken using $\mathbf{g}[220]$ reflection additionally reveals a fine needle-like contrast ($\sim 1.5 - 2.1$ nm) (Figure 1(b)).

In order to investigate the diffracted intensity distribution in reciprocal space, we performed detailed TED examinations. It should be stressed that the main characteristic features observed in the plan-view and the cross-sectional TED patterns are very similar for all $\text{GaP}_y\text{Sb}_{1-y}$ layers grown at different temperatures and growth rates, although there are small differences, depending on the growth temperature, the growth rate and layer composition. The intensity of diffuse streaks pass-

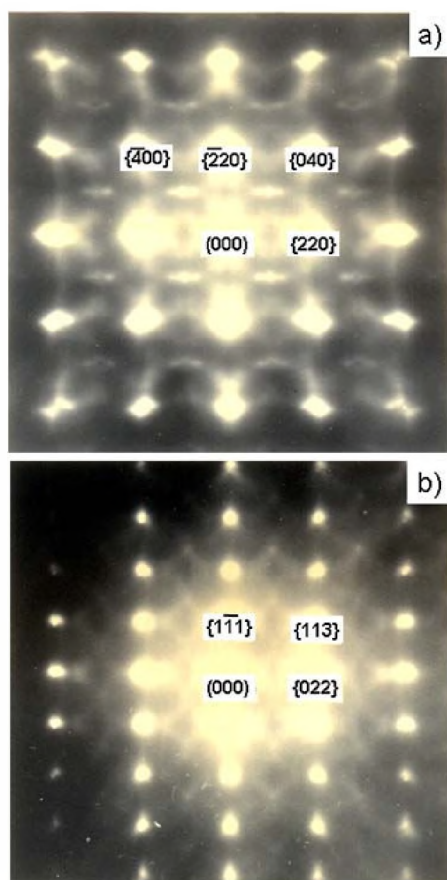


Fig. 2. (a) [001] and (b) [112] TED patterns obtained from a $\text{GaP}_{0.75}\text{Sb}_{0.25}$ layer grown at 560°C and 0.56 nm/s .

ing through the main spots depends on the growth temperature and the composition. Typical results obtained from a $\text{GaP}_{0.75}\text{Sb}_{0.25}$ layer grown at 560°C and 0.56 nm/s are as follows:

The [001] TED pattern is complicated, as shown in Figure 2(a). The standard array of main spots associated with the zinc-blende-type structure is present. The $\{200\}$ spots are weak, which is consistent with the calculated difference of atomic scattering factors between GaP and GaSb. The other main features for the [001] pole TED pattern are i) lines of the [110]-oriented diffuse intensity, ii) diffuse streaks passing through the fundamental reflections and elongated along the [110] direction, iii) extra spots at $\pm 1/4\mathbf{g}[220]$ positions, and iv) a [010]-oriented diffuse intensity with a spacing of $\pm 1/6\mathbf{g}[040]$. The lines of the [110]-oriented diffuse intensity pass close to, but not through, the main spots. These [110]-oriented lines of diffuse intensity correspond to the intersection of the Ewald sphere with planes of diffuse intensity perpendicular to all $\langle 110 \rangle$ directions of the crystal. The intensity varies with position and has a maximum intensity near the main diffraction spots. The extra spots at the $\pm 1/4\mathbf{g}[220]$ positions seem to be due to the intersection

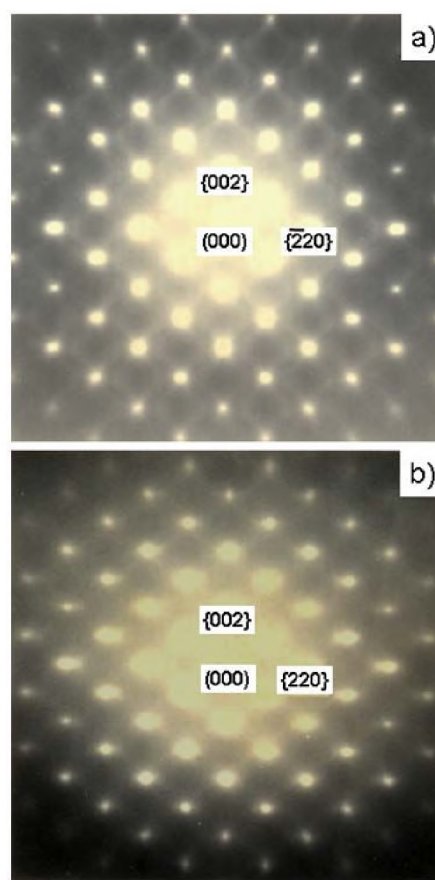


Fig. 3. (a) [110] and (b) [-110] TED patterns obtained from a $\text{GaP}_{0.75}\text{Sb}_{0.25}$ layer grown at 560°C and 0.56 nm/s .

of the Ewald sphere with the [110]-oriented diffuse intensity along the [001] direction. The TEM investigation of the InPSb layers [17] showed that such extra spots associated with [110]-diffuse streaks are related to disc-shaped aggregations of atoms, namely, the fine needle-like TEM contrast, Figure 1(b). The [112] TED pattern is illustrated in Figure 2(b) and exhibits hexagonally-shaped diffuse intensity aligned long the [1-11] direction. The maxima in intensity are located at the $\pm 1/4\mathbf{g}[220]$ and $\pm 1/4\mathbf{g}[111]$ positions.

For the [110] TED pattern, Figure 3(a), the higher order spots are elongated along the [001] and the [-110] directions, and a hexagonally-shaped diffuse intensity occurs along the [001] direction. For the [-110] TED pattern, Figure 3(b), a diffuse streak through the fundamental spots is present and elongated along the [110] direction; its length corresponds to the width of the fine needle-like structure visible in TEM images observed from the [-110] cross-sectional specimen, (*e.g.*, see Figure 1(b)). Higher-order spots are also elongated along the [001] direction and fine diffuse lines are present running through the main spots along the [111] and the [1-1] directions.

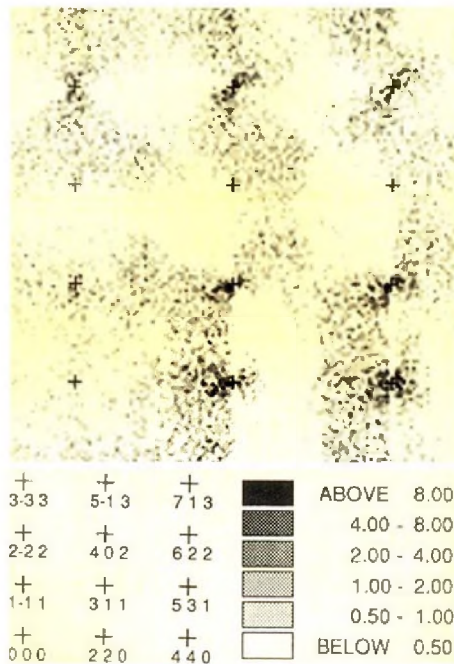


Fig. 4. Calculated distribution of diffuse intensity in a quadrant of a $[1-12]$ reciprocal plane for the $\text{GaP}_{0.75}\text{Sb}_{0.25}$ layer grown at 560°C and 0.56 nm/s .

The characteristic features in the TED patterns of the $\text{GaP}_y\text{Sb}_{1-y}$ layers are different from those reported by Glas *et al.* [18] for InGaAs . They reported only the presence of $\{110\}$ -oriented diffuse lines. As discussed by Glas *et al.* [18], one of the main features revealed by TED examinations is that the maxima in the intensity of the $[110]$ diffuse lines are located away from the main diffraction spots. This indicates that these characteristic features are not associated with phonon scattering, (*i.e.*, similar $[110]$ -oriented diffuse lines can occur as a result of phonon scattering), but in this case, pass exactly through the main diffraction spots [19]. In addition to the $[110]$ -oriented diffuse lines, other complicated features are revealed by the TED investigations. Diffuse streaks, elongated along the $[110]$ direction, are present in the $[001]$ and the $[-110]$ TED patterns, Figures 2(a) and Figure 3(b), respectively, which are thought to be similar to those for $\text{InP}_y\text{Sb}_{1-y}$ layers [17]. These may also arise from segregation, which may be due to stresses associated with surface reconstruction.

In order to understand the origin of the diffuse lines, we calculated the structure of $\text{GaP}_{0.75}\text{Sb}_{0.25}$ (grown at 560°C and 0.56 nm/s) by using the Valence Force Field (VFF) model of Keating [20] and Martin [21], which is known to yield distributions of interatomic distances compatible with the extended X-ray absorption fine structure (EXAFS) results for disordered ternary alloys [22]. The design of the model took into consideration the ease in which the excess energy of a given distribution of atoms was displaced from their virtual crystal

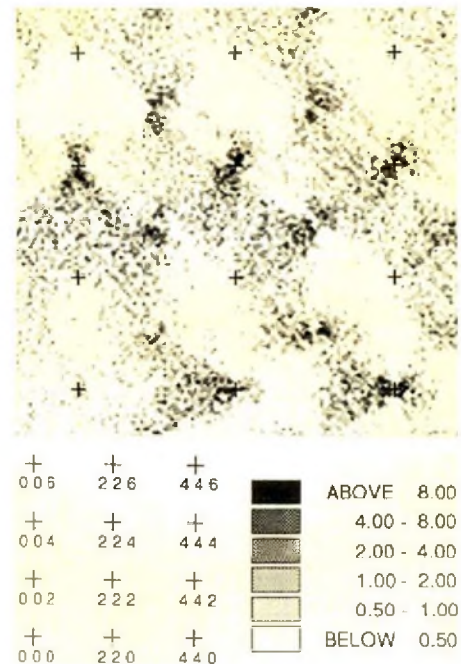


Fig. 5. Calculated distribution of diffuse intensity in a quadrant of a $[1-10]$ reciprocal plane for the $\text{GaP}_{0.75}\text{Sb}_{0.25}$ layer grown at 560°C and 0.56 nm/s .

(VC) sites in a ternary alloy. The details of the crystal model and computer simulations have been reported elsewhere [23]. Figure 4 shows the calculated distribution of the diffuse intensity in a quadrant of a $[1-12]$ reciprocal plane for the $\text{GaP}_{0.75}\text{Sb}_{0.25}$ layer (grown at 560°C and 0.56 nm/s). The grey scales have been adjusted so that the smoothly decreasing background arising from random disorder is almost entirely included in the first grey level. A part of the main features is reproduced. A hexagonally-shaped diffuse intensity is present along the $[1-11]$ direction.

Figure 5 exhibits the calculated distribution of the diffuse intensity in a quadrant of a $[1-10]$ reciprocal plane for the $\text{GaP}_{0.75}\text{Sb}_{0.25}$ layer (grown at 560°C and 0.56 nm/s). The elongation of high-order spots observed in the $[1-10]$ experimental diffraction pattern is reproduced: high order spots are elongated in the $[001]$ and the $[110]$ directions. However, the diffuse streaks passing through the fundamental spots, parallel to the $[110]$ direction, are not reproduced, indicating that they are not associated with a statistically random distribution of atoms on the mixed Group V sublattice, but are due to another source, such as thin disc-type segregation of atoms, as described for the $\text{InP}_y\text{Sb}_{1-y}$ layers [17]. Better agreement between the experimental and the calculated diffraction patterns would undoubtedly have occurred if in the simulations the effects of the fine needle-like contrast visible in the (220) and the (002) TEM DF images had been included. In addition, there is relatively strong intensity at the

{111} position. However, the {111} intensity cannot be distinguished from the {111} main spots of the experimental pattern because they overlap each other.

The results obtained by TED examinations and simulations show that the observed distributions of diffuse intensity are partially consistent with random disorder. Consideration of random disorder leads to possible points that may be related to atomic configuration behavior, *i.e.*, deviation from mean virtual crystal sites even in a perfectly disordered alloy and atomic random distributions of atoms in mixed sublattices. It is noteworthy that the observed [110]-oriented diffuse lines could arise from a static displacement of the sites of the mixed sublattices. Glas [23] demonstrated that in InGaAs, the result of simulations of the displacements associated with chains of 2 or 3 In atoms in a GaAs matrix is consistent with those of the experimental observations. Likewise, in GaPSb, a number of short random chains of P or Sb atoms might be predicted. The random chains and the atomic displacements induced by atoms along the $\langle 110 \rangle$ directions could result in the $\langle 110 \rangle$ -oriented diffuse lines.

IV. SUMMARY

TEM and TED examinations were used to investigate the characteristic features observed in the plan-view and the cross-sectional TED patterns from OMVPE GaPSb layers grown in the range 460 to 500 °C at growth rates of 0.56 and 0.83 nm/s. TEM results showed that a fine-scale modulated contrast (15 – 20 nm) and a fine-scale speckled contrast (~ 5 nm) were present simultaneously. In addition, a fine needle-like contrast ($\sim 1.5 - 2.1$ nm) was observed. The TED results revealed complicated diffracted diffuse intensities. Simulations using the Valence Force Field model indicated that the observed distributions of diffuse intensity were partially consistent with random disorder and that a static displacement of the sites of the mixed sublattices could be responsible for the [110]-oriented diffuse lines.

REFERENCES

- [1] B. H. Koo, G. B. Chon, H. S. Lim, C. G. Lee and T. Yao, *J. Korean Phys. Soc.* **49**, 873 (2006).
- [2] S. W. Chae, J. S. Kwak, S. K. Yoon, M. Y. Kim, J. O. Song, T. Y. Seong, and T. G. Kim, *J. Korean Phys. Soc.* **49**, 899 (2006).
- [3] B. de Cremoux, *J. de Physique C* **5**, suppl. No 12, C5-19 (1982).
- [4] K. Onabe, *Jpn. J. Appl. Phys.* **21**, 964 (1982).
- [5] G. B. Stringfellow, *J. Cryst. Growth* **54**, 404 (1983).
- [6] K. Ishida, T. Shumiya, T. Nomura, H. Ohtani and T. Nishizawa, *J. Less-Common Metals* **142**, 135 (1988).
- [7] A. G. Norman and G. R. Booker, *J. Appl. Phys.* **57**, 4715 (1985).
- [8] A. G. Norman and G. R. Booker, *Inst. Phys. Conf. Ser.* **76**, 257 (1985).
- [9] S. N. G. Chu, S. Nakahara, K. E. Strege and W. D. Johnston, *J. Appl. Phys.* **57**, 4610 (1985).
- [10] M. Quillec, J. L. Benchimol, S. Slemkes and H. Launois, *Appl. Phys. Lett.* **42**, 886 (1983).
- [11] T.-Y. Seong, G. R. Booker and A. G. Norman, *Inst. Phys. Conf. Ser.* **134**, 301 (1993).
- [12] F. Glas, C. Gors and P. Henoc, *Phil. Mag.* **B62**, 373 (1990).
- [13] P. Blood and A. D. C. Grassie, *J. Appl. Phys.* **56**, 1866 (1984).
- [14] J. S. Roberts, G. B. Scotts and J. P. Gowers, *J. Appl. Phys.* **52**, 4018 (1981).
- [15] C. P. Kuo, R. M. Cohen and G. B. Stringfellow, *J. Cryst. Growth* **64**, 461 (1983).
- [16] J. Taftt and J. H. L Spence, *J. Appl. Cryst.* **15**, 60 (1982).
- [17] T.-Y. Seong, G. R. Booker, A. G. Norman and G. B. Stringfellow, *Jpn. J. Appl. Phys.* (to be published).
- [18] F. Glas, C. Gors and P. Henoc, *Phil. Mag.* **B62**, 373 (1990).
- [19] C. H. Narayanan and S. M. Copley, *Phys. Stat. Sol. A* **23**, 123 (1974).
- [20] P. N. Keating, *Phys. Rev.* **145**, 637 (1966).
- [21] R. M. Martin, *Phys. Rev. B* **1**, 4005 (1970).
- [22] Y. Zhu, M. Suenaga and A. R. Moodenbaugh, *Phil. Mag. Lett.* **62**, 51 (1990).
- [23] F. Glas, *Inst. Phys. Conf. Ser.* **100**, 167 (1989).